Archives of Academic Emergency Medicine. 2026; 14(1): e41

OPEN ACCESS

ORIGINAL RESEARCH

Modulatory Effects of Methadone on Brain Network Instability in Methamphetamine Use; A Cross-sectional Study

Javad Sheikhi Koohsar[1], Sadegh Masjoodi[2], Farzad Ashrafi[3], Mehran Arab-Ahmadi[4], Babak Jamshidi[5], Amir Khorasani[6], Alireza Azizi[7], Melika Boroomand-Saboor[8], Shahriyar Jamshidi Zargaran[1], Mohammad Bagher Tavakoli[9]*

1. Department of Bioimaging, School of Advanced Technologies in Medicine, Isfahan University of Medical Sciences, Isfahan, Iran
2. Shiraz Neuroscience Research Center, Assistant Professor, Medical Engineering, Shiraz University of Medical Sciences, Iran
3. Neurology department, Shahid Beheshti University of Medical Sciences, Tehran, Iran
4. Advanced Diagnostic and Interventional Radiology Research Center, Tehran University of Medical Sciences, Tehran, Iran
5. Medical Statistician, KiTEC, King's College London, London, UK
6. Department of Bioimaging, School of Advanced Technologies in Medicine, Isfahan University of Medical Sciences, Isfahan, Iran
7. Department of Neuroscience, Shahroud University of Medical Sciences, Shahroud, Iran
8. Faculty of Medicine, Shahid Beheshti University of Medical Sciences, Tehran, Iran
9. Department of Medical Physics, School of Medicine, Isfahan University of Medical Sciences, Isfahan, Iran

Received: May 2026; Accepted: June 2026; Published online: 22 August 2026

Abstract: **Introduction:** While methadone maintenance therapy (MMT) is well established in opioid use disorder, its potential modulatory effects on brain network dynamics in methamphetamine use disorder (MUD) remain unclear. This study aimed to evaluate the association of MMT with normalization of disrupted brain network activity in MUD.

Methods: In this cross-sectional study, resting-state functional magnetic resonance imaging (MRI) data were obtained from healthy controls, untreated methamphetamine users, and methamphetamine users receiving MMT who also met diagnostic criteria for opioid use disorder and were enrolled in supervised MMT programs. Dynamic functional connectivity was assessed using dynamic independent component analysis within the CONN toolbox. Clinical status was evaluated using the Positive and Negative Syndrome Scale (PANSS) and Brief Assessment of Cognition in Schizophrenia (BACS). Group comparisons were performed using general linear models controlling for age, education level, duration of methamphetamine use, and head-motion parameters. **Results:** 110 participants (35 healthy controls, 45 untreated individuals with methamphetamine use, and 30 individuals with methamphetamine use receiving MMT) were studied. Cognitive performance assessed using BACS differed significantly across groups ($p = 0.002$, $\eta^2 = 0.332$), with untreated methamphetamine users demonstrating the lowest scores (19.88 ± 6.20), healthy controls the highest scores (30.38 ± 5.85), and MMT-treated participants showing intermediate performance (22.48 ± 7.61). Compared with untreated methamphetamine users, MMT-treated participants showed higher BACS scores, although the methamphetamine versus MMT effect was small-to-moderate (Cohen's d = -0.38, 95% confidence interval (CI): -0.85 to 0.08). PANSS positive, negative, and general psychopathology scores differed significantly across groups (all $p < 0.001$), with large effect sizes (η^2 range = 0.802–0.913). Untreated methamphetamine users exhibited the greatest symptom severity (Cohen's d = 2.74, 95% CI: 2.10–3.38), whereas MMT-treated participants showed lower symptom burden than untreated users (Cohen's d = 2.26, 95% CI: 1.67–2.85), although scores remained elevated relative to healthy controls (d = 4.22, 95% CI: 3.34, 5.11). The methamphetamine versus MMT effect sizes were large for PANSS positive (Cohen's d = 2.74, 95% CI: 2.10–3.38), PANSS negative (Cohen's d = 2.26, 95% CI: 1.67–2.85), and PANSS general psychopathology (Cohen's d = 1.64, 95% CI: 1.11–2.18).

Conclusion: Methamphetamine use is associated with disrupted and unstable brain network dynamics that may underlie acute neurobehavioral disturbances seen in emergency settings. MMT was associated with partial stabilization of these alterations, suggesting a potential neurobiological benefit beyond opioid substitution. Persistent network abnormalities, however, indicate the need for adjunctive therapeutic strategies. Dynamic connectivity measures may offer a novel biomarker for risk stratification and management of substance-related emergencies.

Keywords: Amphetamine-related disorders; Opiate substitution treatment; Functional neuroimaging; Connectome

Cite this article as: Sheikhi Koohsar J, Masjoodi J, Ashrafi F, et al. Modulatory Effects of Methadone on Brain Network Instability in Methamphetamine Use; A Cross-sectional Study. Arch Acad Emerg Med. 2026; 14(1): e41. https://doi.org/10.22037/aaem.v14i1.3050.

***Corresponding Author:** Mohammad Bagher Tavakoli; School of Medicine, Isfahan University of Medical Sciences, Hezar Jerib Avenue, Isfahan, Iran. Postal Code: 8174673461, Tel: 00983137929012, Email: mbtavakoli@mui.ac.ir, ORCID: https://orcid.org/0000-0001-8721-4922.

This open-access article distributed under the terms of the Creative Commons Attribution NonCommercial 3.0 License (CC BY-NC 3.0).
Downloaded from: https://journals.sbmu.ac.ir/aaem/index.php/AAEM/index

1. Introduction

Methamphetamine use disorder (MUD) is a significant public health problem characterized by neurocognitive impairment, psychotic symptoms, and high rates of relapse(1). Chronic methamphetamine exposure disrupts dopaminergic and glutamatergic neurotransmission, leading to changes in functional connectivity (FC) in brain networks involved in cognitive control, emotional regulation, and sensory integration(2). While pharmacological interventions such as methadone maintenance therapy (MMT) have shown efficacy in opioid addiction, their potential effects on methamphetamine-associated cognitive and psychotic impairments remain poorly understood (3). Recent advances in dynamic connectivity analysis using resting-state functional magnetic resonance imaging (rs-fMRI) offer a new lens to study temporally varying network interactions and provide deeper insights into the neural mechanisms of addiction and recovery(4).

Methamphetamine-associated psychosis (MAP) has clinical similarities to schizophrenia, including hallucinations, delusions, and thought disorder, but arises from a different neurobiological pathway. In resting-state fMRI studies, methamphetamine users were found to have aberrant connectivity in the default mode network (DMN), salience network (SN), and frontoparietal network (FPN), with cross-network hypoconnectivity (e.g., DMN-FPN) correlating with the severity of positive symptoms on the Positive and Negative Syndrome Scale (PANSS)(5). For example, reduced connectivity between the sensory-somatomotor network (SMN) and attention networks has been associated with impaired sensory integration and attention deficits in MAP. These findings emphasize the role of large-scale network dysregulation in methamphetamine-related psychosis, but most studies focus on static FC and neglect the temporal dynamics of network interactions that might better reflect fluctuating cognitive states and symptom severity(6, 7).

While MMT is a cornerstone of treatment for opioid dependence, its applicability to methamphetamine use disorder is less clear(8). Emerging evidence suggests that neuromodulatory interventions such as repetitive transcranial magnetic stimulation (rTMS) can normalize FC patterns in addiction-related networks, particularly in the prefrontal cortex and reward circuits(9). For example, rTMS has been shown to increase beta-band connectivity and improve cognitive outcomes in methamphetamine users, emphasizing the potential for targeted therapies to restore network efficiency. Similarly, MMT may have similar effects by normalizing neurotransmitter systems, although its effects on dynamic network reconfiguration remain unexplored(10).

Conventional rs-fMRI analyses often overlook the millisecond fluctuations in FC that characterize real brain function. Dynamic connectivity approaches, on the other hand, capture transient network states and provide a more nuanced understanding of addiction-related dysregulation(11). For example, EEG microstate studies in methamphetamine users show impaired temporal dynamics in microstate classes A (auditory processing) and B (visual attention), which correlate with attention bias and drug use history(12). Transferring these results to fMRI, dynamic connectivity could shed light on how methamphetamine and MMT modulate transient network interactions, such as the uncoupling of DMN and SMN during cognitive tasks, or normalize aberrant connections associated with psychosis(13).

This study employed dynamic functional connectivity (dFC) analyses within the CONN toolbox framework to compare large-scale brain network dynamics among untreated methamphetamine users, methamphetamine users receiving MMT, and age-matched healthy controls. In addition, associations between dynamic connectivity alterations, cognitive performance, and psychotic symptom severity were investigated to identify potential neuroimaging biomarkers of treatment response and neurobehavioral dysfunction.

2. Methods

2.1. Study design and setting

In this cross-sectional study, long-term methamphetamine-dependent subjects were analyzed together with healthy, age-matched control subjects. Methamphetamine-dependent participants were recruited between 2024 and late 2025 from MMT clinics and emergency departments (EDs) affiliated with Shahroud University of Medical Sciences, Iran. Participants with methamphetamine use met DSM-5 criteria for methamphetamine use disorder(14). MMT participants also met clinical criteria for opioid use disorder and were enrolled in supervised methadone maintenance programs.

To address important gaps in the current literature, we: (A) compare the dynamic connectivity patterns of untreated methamphetamine users, MMT-treated patients, and controls using a validated dynamic independent component analysis(dICA) approach in the CONN framework; and (B) assess the extent to which MMT modulates large-scale network dynamics and attenuates psychotic symptoms as measured by the Positive and Negative Syndrome Scale (PANSS), supporting its potential neuroregulatory effect in stimulant dependence. Healthy control subjects were screened to ensure that no substance use disorders or other medical or neurological conditions were present. Written informed consent was obtained from all participants, and ethical approval was granted by the Ethics Committee of Isfahan University of Medical Sciences (IR.MUI.MED.REC.1402.453).

2.2. Participants

Healthy controls were age-matched participants with no substance use disorder, neurological disorder, chronic systemic illness, or contraindication to MRI. The inclusion criteria for participants with methamphetamine use disorder were age between 25 and 40 years and methamphetamine

This open-access article distributed under the terms of the Creative Commons Attribution NonCommercial 3.0 License (CC BY-NC 3.0).
Downloaded from: https://journals.sbmu.ac.ir/aaem/index.php/AAEM/index

use for more than five years. Participants in the MMT group had maintained abstinence from methamphetamine for approximately two months before imaging. In contrast, participants in the untreated METH group had recent methamphetamine use confirmed by urine screening. Participants in the untreated METH group were not receiving methadone maintenance therapy or other regular psychoactive medications at the time of assessment. All participants provided written informed consent in accordance with the Institutional Review Board.

Participants receiving MMT were additionally screened for opioid use disorder through structured clinical interviews and treatment records obtained from affiliated methadone maintenance clinics. Enrollment in an active MMT program was verified through medical documentation. Although MMT participants had maintained abstinence for at least two months before imaging, previous studies suggest that methamphetamine-associated neurobiological alterations, cognitive deficits, and psychotic symptoms may persist long after cessation of drug use. Therefore, the present findings are interpreted as reflecting enduring neurofunctional consequences of prior methamphetamine exposure rather than acute drug effects.

Participants receiving methadone maintenance therapy were treated with a stable maintenance dose ranging from 60 to 90 mg/day (mean: 72 ± 15 mg/day) for a minimum of eight weeks before MRI acquisition.

2.3. Data gathering and measurements

Demographic data were collected for all participants, including age, education level, and duration of methamphetamine use. Right-handedness was confirmed using the Edinburgh Handedness Inventory. Methamphetamine dependence was validated by a rapid urine test with a detection limit of ≥500 ng/ml.

Standardized clinical instruments were used to assess participants' psychological and cognitive status, including PANSS, which quantifies symptom severity across psychotic domains. These measures were used to explore associations between clinical outcomes and dynamic connectivity patterns(15), as well as the Brief Assessment of Cognition in Schizophrenia (BACS)(16), which assesses verbal memory, working memory, motor speed, fluency, attention, and executive function.

MMT participants had received methadone for a minimum of eight weeks before MRI acquisition. Methadone treatment status was verified using clinical treatment records. Treatment adherence and continuity were confirmed via clinic documentation.

2.4. Image acquisition and analysis

Functional and anatomical images were acquired using a Siemens 1.5T Avanto MRI scanner with an 18-channel head coil. Resting-state fMRI parameters (rs-fMRI) included Repetition Time (TR) = 3300 ms, Time to Echo (TE) = 45 ms, slice thickness = 3.5 mm, and matrix size = 64×64, with 200 measurements over 11 minutes. T1-weighted structural data were collected with TR = 2400 ms, TE = 3.79 ms, and slice thickness = 1.2 mm. Participants were instructed to remain awake and close their eyes during the scans. Analyses of the fMRI data were performed using CONN(17).(RRID: SCR_009550) release 22.v2407(18) and SPM12 (19) (RRID: $SCR_0 07037) Release 12.7771 in MATLAB R2018b$.

2.5. Preprocessing

The anatomical data were segmented into the tissue classes grey matter, white matter, and cerebrospinal fluid using the uniform segmentation and normalization algorithm SPM12(20) (21) With the default IXI-549 tissue probability map template.

2.6. Denoising

In addition, the functional data were denoised using a standard denoising pipeline(22) including regression of potential confounding effects introduced by white matter time series (5 component based noise correction method (CompCor) noise components), cerebrospinal fluid (CSF) time series (5 CompCor noise components), session effects and their first-order derivatives (2 factors), and linear trends (2 factors) within each functional run, followed by bandpass frequency filtering of the blood oxygenation level-dependent (BOLD) time series(23, 24) between 0.008 Hz and 0.09 Hz. CompCor(25) . The noise components within the white matter and CSF were estimated by calculating the average BOLD signal and the largest principal components orthogonal to the BOLD average within the eroded segmentation masks of each subject. Based on the number of noise terms included in this denoising strategy, the effective degrees of freedom of the BOLD signal after denoising were estimated to be 91.5 to 100.7 (average 100.4) across all subjects(26).

2.7. First-level analysis RRC_01

Dynamic independent component analyses (dyn-ICA)(22) were performed to estimate the first 10 temporal modulation factors that characterize the observed dynamic changes in functional connectivity within each functional run, together with the circuits (groups of connections) modulated by each of these factors. Blood oxygen level-dependent (BOLD) time series were extracted from predefined regions of interest (ROIs) Human Connectome Project independent component analysis (HCP-ICA) networks (17) and Harvard-Oxford Atlas ROI(27)were concatenated across all subjects. Functional connectivity between each pair of regions was modelled by a generalized psychophysiological interaction model (gPPI)(28, 29). With 10 unknown psychological factors and an interactive dual regression algorithm using a Hanning regularization kernel with a 30s full-width half maximum (FWHM), maximum likelihood estimates of these factors were computed. Finally, a fast-ICA fixed-point algorithm(30). The hyperbolic tangent contrast function was ap-

This open-access article distributed under the terms of the Creative Commons Attribution NonCommercial 3.0 License (CC BY-NC 3.0).
Downloaded from: https://journals.sbmu.ac.ir/aaem/index.php/AAEM/index

plied to the regression coefficients of the resulting group-level gPPI model interaction terms to identify spatially independent group-level circuits. A separate gPPI model was used for each subject to compute subject-specific ICA maps associated with the same circuits.

2.8. Second-level analysis RRC_02

Group-level analyses were performed using general linear models (GLM). Age, education level, duration of methamphetamine use, and head-motion parameters were included as covariates where appropriate to minimize potential confounding effects. In addition to p-values, effect sizes and 95% confidence intervals (CIs) were calculated to facilitate interpretation of the magnitude of group differences(31). A separate GLM was estimated for each compound, with first-level connectivity measures at that compound as dependent variables (one independent sample per subject and one measure per task or experimental condition, if applicable) and subject-level groups or other identifiers as independent variables. Link-level hypotheses were assessed using multivariate parametric statistics with random effects between subjects and covariance estimation for the sample across measures. Inferences were made at the individual cluster level (groups of similar compounds). Cluster-level inference was based on parametric statistics within and between each pair of networks (functional network connectivity)(32), where the networks were identified using a hierarchical clustering method with complete linkage(33). based on the anatomical proximity of ROI to ROI and functional similarity metrics(18). The results were assessed using a combination of a threshold of $p < 0.05$ at the linkage level and a family-wise corrected threshold of p-FDR < 0.05 at the cluster level(34).

2.9. Statistical analysis

Sample size was determined based on feasibility and previous resting-state fMRI studies in substance use disorders reporting medium-to-large effect sizes. A post-hoc power analysis indicated that the current sample (n = 110) provided greater than 80% statistical power to detect medium effect sizes (Cohen's $d \geq 0.50$) at = 0.05.

Group differences in demographic, cognitive, and clinical variables were assessed using one-way analysis of variance (ANOVA) for continuous variables and ² tests for categorical variables. Homogeneity of variance was evaluated using Levene's test. Post hoc comparisons were performed using Tukey's honestly significant difference (HSD) test when appropriate. Covariates included age, education, duration of methamphetamine use, and head-motion parameters. The sample size (n = 110) provided adequate statistical power (>80%) to detect medium effect sizes at = 0.05 based on prior neuroimaging studies of methamphetamine use disorder. Statistical analyses were conducted using SPSS version 26 and MATLAB R2020a.

3. Results

3.1. Clinical and demographic characteristics

This cross-sectional study recruited 110 participants: 35 healthy controls, 45 untreated individuals with methamphetamine use, and 30 individuals with methamphetamine use receiving MMT. Table 1 compares the demographic, cognitive, and clinical characteristics of the studied participants. Significant group differences were observed in cognitive and psychopathological measures. Cognitive performance assessed using BACS differed significantly across groups ($p = 0.002$, $\eta^2 = 0.332$), with untreated methamphetamine users demonstrating the lowest scores (19.88 ± 6.20), healthy controls the highest scores (30.38 ± 5.85), and MMT-treated participants showing intermediate performance (22.48 ± 7.61). Compared with untreated methamphetamine users, MMT-treated participants showed higher BACS scores, although the methamphetamine versus MMT effect was small-to-moderate (Cohen's d = -0.38, 95% CI: -0.85 to 0.08).

PANSS positive, negative, and general psychopathology scores differed significantly across groups (all $p < 0.001$), with large effect sizes (η^2 range = 0.802–0.913). Untreated methamphetamine users exhibited the greatest symptom severity (Cohen's d = 2.74, 95% CI: 2.10–3.38), whereas MMT-treated participants showed lower symptom burden than untreated users (Cohen's d = 2.26, 95% CI: 1.67–2.85), although scores remained elevated relative to healthy controls (d = 4.22, 95% CI: 3.34, 5.11). The methamphetamine versus MMT effect sizes were large for PANSS positive (Cohen's d = 2.74, 95% CI: 2.10–3.38), PANSS Negative (Cohen's d = 2.26, 95% CI: 1.67–2.85), and PANSS General Psychopathology (Cohen's d = 1.64, 95% CI: 1.11–2.18).

3.2. ROI to ROI dynamic independent analysis

This study was an exploratory research with a small sample size examining dynamic functional connectivity differences associated with MMT for methamphetamine dependence over an eight-week post-treatment period from the perspective of dynamic functional connectivity assessed across 10 dynamic conditions using the CONN toolbox.

Subjects included methamphetamine abusers and MMT post-treatment subjects who were compared to age-matched healthy controls in the dynamic functional connectivity domain. The results showed contrasts between subjects in Group A (healthy controls and methamphetamine users) (Figure 1) across components 1, 4, 6, and 8, along with the corresponding effect sizes for each cluster. Independent component (IC)1 showed a significant difference between the two clusters. Cluster 1 primarily comprises the hippocampus, dorsal attention network, and superior sensorimotor cortex. Cluster 2 includes the default mode PCC, precuneus cortex, medial visual cortex, and temporal fusiform cortex. IC4 showed significant differences in Clusters 2 and 5. Visual Occipital, Cerebellar Anterior, Default Mode MPFC, and Cingulate Gyrus in Cluster 2 and Lingual Gyrus Right,

This open-access article distributed under the terms of the Creative Commons Attribution NonCommercial 3.0 License (CC BY-NC 3.0).
Downloaded from: https://journals.sbmu.ac.ir/aaem/index.php/AAEM/index

Temporal Fusiform Cortex, Occipital Fusiform Gyrus, and Vermis in Cluster 5 change the dynamic connectivity properties. In IC6, we observed significant differences in Cluster 2, which includes the frontoparietal LPFC, temporal fusiform cortex, parahippocampal gyrus, and other regions. In IC8, distinct differences were evident in Clusters 2 and 3: Cluster 2 involved the lateral sensorimotor cortex and language-related areas, while Cluster 3 included the posterior superior temporal gyrus (pSTG) and superior temporal gyrus.

Dynamic connectivity analysis contrasting healthy controls (HC) and treated subjects is presented in Figure 2. Results demonstrate significant between-group differences in independent components IC2, IC3, IC4, IC5, IC6, and IC8 across multiple clusters.

4. Discussion

4.1. Key findings and network implications

The present study demonstrates impaired dynamic functional connectivity (dFC) in methamphetamine users, in both untreated METH and MMT groups, spanning multiple large brain networks. These results emphasize the complexity of addiction-related neuroadaptations and suggest that MMT may have partial restorative effects. Participants in the METH group showed reduced dFC in core regions of the DMN, especially in the posterior cingulate cortex and precuneus, as well as in the hippocampus, compared to healthy controls (HC). The DMN is central to self-referential cognition and introspective awareness; its dysregulation has been repeatedly linked to craving and reduced self-monitoring in methamphetamine use. The changes observed here in the hippocampus may reflect memory impairment caused by methamphetamine neurotoxicity, which is consistent with previous volumetric studies (35, 36). The partial restoration of connectivity in these regions after MMT (Figure 3: MMT vs METH in IC2, IC5) suggests an improvement in internal state regulation. Nevertheless, the persistent deviations compared to HC (Figure 2) indicate remaining impairments and incomplete recovery pathways.

The connectivity of the frontoparietal network (FPN), which is involved in cognitive control and adaptive regulation, was impaired in both the MMT and METH groups. The persistent deficit in MMT subjects suggests that MMT alone is not sufficient to address executive dysfunction, which has been shown to contribute to relapse susceptibility(37). Previous reports confirm that flexibility within FPN is associated with decision-making ability and the sustainability of abstinence(38).

Changes in sensorimotor and language-associated regions, particularly in the superior temporal gyrus (IC8), may be associated with deficits in coordination and social communication. These areas are frequently impaired in stimulant dependence and have been associated with network-level dysconnectivity in both preclinical and clinical studies(39-41). The persistence of these differences after MMT (Figure 2) suggests long-term neurological adaptations that may require multimodal rehabilitation.

The connectivity impairments in the visual and cerebellar circuits (IC4, IC5) are consistent with the neurotoxic profile of methamphetamine. Dysfunction in these regions before treatment reflects impaired sensory integration and motor sequencing. The partial recovery patterns observed in MMT (Figure 3: MMT vs. METH comparison) may reflect either detoxification-induced neuroplasticity or reduced neurochemical burden(13). However, the extent and duration of these improvements remain unclear, given the limited duration of treatment.

4.2. MMT effects and partial normalization

In MMT participants, additional connectivity shifts compared to HCs (IC2, IC3, IC5) suggest that MMT may induce compensatory or adaptive reorganization within the affected circuits(42, 43).

The intermediate connectivity profile observed in the MMT group, which shares features with both METH and HC, opens the possibility of partial normalization, especially in regions involved in affective regulation and interoceptive perception. Although the therapeutic mechanism of MMT in methamphetamine dependence remains uncertain, several hypotheses should be considered. Because participants in the MMT group had comorbid opioid use disorder, methadone may have exerted indirect stabilizing effects via -opioid receptor agonism and downstream modulation of glutamatergic systems(44, 45). Alternatively, off-target effects on dopaminergic pathways could influence reward and stress regulation circuitry, consistent with the observed shifts in SN-DMN coupling following treatment.(46) The observed partial normalization of DMN and cerebellar connectivity in the MMT group suggests that methadone may exert stabilizing effects on intrinsic neural dynamics disrupted by chronic stimulant exposure. However, the persistent abnormalities in the frontoparietal and sensorimotor networks indicate that higher-order executive and motor systems remain vulnerable even after treatment. This pattern aligns with previous findings emphasizing that executive dysfunction in stimulant dependence requires extended recovery periods and often persists despite pharmacological intervention.

Although MMT is not a standard treatment for methamphetamine use disorder, the intermediate connectivity profile of the treated group, positioned between untreated users and healthy controls, suggests potential neuromodulatory impacts on large-scale brain systems. Nevertheless, given the cross-sectional design and relatively short treatment window, these findings should be interpreted cautiously. Complementary therapeutic approaches such as cognitive remediation, neuromodulation, or mindfulness-based interventions may be required to target residual deficits in cognitive control and network flexibility.

Disrupted dynamic functional connectivity in methamphetamine users may underlie acute psychiatric manifesta-

This open-access article distributed under the terms of the Creative Commons Attribution NonCommercial 3.0 License (CC BY-NC 3.0).
Downloaded from: https://journals.sbmu.ac.ir/aaem/index.php/AAEM/index

tions frequently seen in emergency departments, including agitation, psychosis, and impaired decision-making. Partial normalization with MMT suggests that time-resolved connectivity measures could serve as biomarkers to identify high-risk patients, guide early management, and triage interventions. These findings highlight the need for integrating neuroimaging-informed strategies with clinical assessment in acute care settings. Alternative explanations should also be considered. Because treatment assignment was not randomized, baseline differences between treated and untreated participants may have influenced the observed findings. Individuals who engage successfully in MMT programs may differ in motivation, treatment adherence, psychosocial support, or illness severity. These factors could partially account for differences in dynamic connectivity patterns. Furthermore, the selective normalization of default mode and cerebellar networks compared with persistent abnormalities in frontoparietal and sensorimotor systems may reflect differential rates of neurobiological recovery. Networks supporting higher-order executive functions are known to demonstrate prolonged vulnerability following chronic stimulant exposure and may require longer periods of abstinence or adjunctive interventions for recovery. The persistence of abnormalities within executive-control and sensorimotor networks despite treatment may indicate that some methamphetamine-related neural alterations are less responsive to current pharmacological interventions and may require longer recovery periods or complementary therapeutic approaches.

5. Methodological considerations and limitations

This study has several limitations. First, the relatively small sample size may limit statistical power and reduce generalizability. Second, the cross-sectional design precludes causal inference regarding the effects of methadone maintenance therapy on dynamic connectivity alterations. Third, residual confounding related to psychiatric comorbidities, polysubstance exposure, medication history, and environmental factors cannot be completely excluded. Fourth, although extensive denoising procedures and motion correction were applied, resting-state functional connectivity measures remain susceptible to motion-related and physiological artifacts. Finally, the relatively short duration of MMT exposure may not fully capture long-term treatment-related neuroplastic changes. Future longitudinal studies incorporating larger samples and multimodal neuroimaging approaches are warranted. Furthermore, because MMT participants were abstinent at the time of imaging, findings in this group cannot distinguish residual effects of prior methamphetamine exposure from long-term recovery-related neuroadaptations.

6. Clinical and future directions

Establishing robust behavioral correlates of dFC changes would greatly enhance translational relevance. For example, increased ECN flexibility and normalized DMN-SN transitions may correlate with reduced impulsivity, lower craving intensity, and better executive function(47, 48). Multimodal imaging, combining rs-fMRI with DTI, structural MRI, and PET, can elucidate the mechanistic basis of observed changes, including white matter integrity and neurotransmitter receptor availability. Interventions targeting specific networks may complement pharmacological treatment. Mindfulness-based therapies, cognitive control training, and neuromodulation (e.g., tACS, rTMS) have shown potential in restoring DMN-FPN balance and mitigating cue reactivity(36, 49). Together, these findings support a network-level understanding of addiction and recovery. Future work should prioritize longitudinal designs, individualized connectivity profiling, and targeted modulation strategies to optimize outcomes in stimulant use disorder.

7. Conclusions

This study provides evidence that methamphetamine use disorder is associated with substantial disturbances in dynamic functional connectivity across multiple large-scale brain networks. Participants receiving methadone maintenance therapy demonstrated partial normalization of several connectivity abnormalities, particularly within default mode and cerebellar systems, accompanied by improvements in cognitive performance and psychotic symptoms. Nevertheless, persistent dysfunction within executive and sensorimotor networks suggests that methadone alone may not fully reverse the neurobiological consequences of chronic methamphetamine exposure. While dynamic connectivity measures show promise as potential biomarkers of treatment response and disease severity, further longitudinal investigations are required before these findings can be translated into routine clinical practice or emergency medicine decision-making.

8. Declarations

8.1. Acknowledgments

The authors thank all participants and clinical/radiology staff involved in data collection.

8.2. Authors' Contribution

All authors contributed to the manuscript preparation. JK, HK, and MT designed and conceptualized the study; JK, SJ, AA, FA, MB, and MA recruited the participants and completed the screening assessments. JK, SM, AA, and BJ analyzed the data and performed the statistical analysis. JK, MA, FA, SM, MB, and MT wrote the initial draft of this manuscript. MT acquired funding, and the final manuscript was approved by all the authors.

This open-access article distributed under the terms of the Creative Commons Attribution NonCommercial 3.0 License (CC BY-NC 3.0).
Downloaded from: https://journals.sbmu.ac.ir/aaem/index.php/AAEM/index

8.3. Ethical considerations

The study was approved by the Research Ethics Committees of the School of Medicine - Isfahan University of Medical Sciences (Approval number IR.MUI.MED.REC.1402.453). Approval Date: 2024-03-05.

8.4. Conflict of interest

The authors declare no potential conflicts of interest regarding this article's research, authorship, and/or publication.

8.5. Funding and supports

This work was supported by Isfahan University of Medical Sciences, Isfahan, Iran. Mohammad Bagher Tavakoli acquired the funding.

8.6. Data availability

Individual-level imaging data are not publicly available because of ethics and privacy restrictions. De-identified derived features and analysis scripts may be made available from the corresponding author upon reasonable request and is subject to institutional approval.

8.7. Using artificial intelligence chatbots

During preparation of this work, the authors used AI-assisted language support to improve Figures, Table and journal formatting. The authors reviewed and edited all content as needed and take full responsibility for the content of the submitted manuscript.

References

1. Rusyniak DE. Neurologic manifestations of chronic methamphetamine abuse. Psychiatr Clin North Am. 2013;36(2):261–75.
2. Bernheim A, See RE, Reichel CM. Chronic methamphetamine self-administration disrupts cortical control of cognition. Neurosci Biobehav Rev. 2016;69:36–48.
3. Shariatirad S, Maarefvand M, Ekhtiari H. Methamphetamine use and methadone maintenance treatment: an emerging problem in the drug addiction treatment network in Iran. Int J Drug Policy. 2013;24(6):e115–e6.
4. Larrivee D. Resting-State fMRI Advances for Functional Brain Dynamics. In: Larrivee D, editor. New Advances in Magnetic Resonance Imaging. London: IntechOpen; 2024.
5. Wearne TA, Cornish JL. A comparison of methamphetamine-induced psychosis and schizophrenia: a review of positive, negative, and cognitive symptomatology. Front Psychiatry. 2018;9:491.
6. Ipser JC, Uhlmann A, Taylor P, Harvey BH, Wilson D, Stein DJ. Distinct intrinsic functional brain network abnormalities in methamphetamine-dependent patients with and without a history of psychosis. Addict Biol. 2018;23(1):347–58.
7. Hwang ZA, Hsu AL, Li CW, Wu CW, Chen CH, Chan WP, et al. The distinct functional brain network and its association with psychotic symptom severity in men with methamphetamine-associated psychosis. BMC Psychiatry. 2024;24(1):671.Radfar SR, Cousins SJ, Shariatirad S, Noroozi A, Rawson RA. Methamphetamine use among patients undergoing methadone maintenance treatment in Iran; a threat for harm reduction and treatment strategies: a qualitative study. Int J High Risk Behav Addict. 2016;5(4):e30327.Dorsey ER, Topol EJ. Telemedicine 2020 and the next decade. Lancet. 2020;395(10227):859.
8. Han X, Zhu Z, Luan J, Lv P, Xin X, Zhang X, et al. Effects of repetitive transcranial magnetic stimulation and their underlying neural mechanisms evaluated with magnetic resonance imaging-based brain connectivity network analyses. Eur J Radiol Open. 2023;10:100495.
9. Li Y, Yang B, Ma J, Li Y, Zeng H, Zhang J. Assessment of rTMS treatment effects for methamphetamine addiction based on EEG functional connectivity. Cogn Neurodyn. 2024;18(5):2373–86.
10. Scarapicchia V, Kwan H, Czippel A, Gawryluk JR. Differences Between Resting-State fMRI BOLD Variability and Default Mode Network Connectivity in Healthy Older and Younger Adults. Brain Connect. 2024;14(7):391–8.
11. Chen T, Su H, Zhong N, Tan H, Li X, Meng Y, et al. Disrupted brain network dynamics and cognitive functions in methamphetamine use disorder: insights from EEG microstates. BMC Psychiatry. 2020;20(1):334.
12. Ishida T, Nakamura Y, Tanaka SC, Mitsuyama Y, Yokoyama S, Shinzato H, et al. Aberrant Large-Scale Network Interactions Across Psychiatric Disorders Revealed by Large-Sample Multi-Site Resting-State Functional Magnetic Resonance Imaging Datasets. Schizophr Bull. 2023;49(4):933–43.
13. American Psychiatric A. Diagnostic and Statistical Manual of Mental Disorders, Text Revision (DSM-5-TR). 5 ed. Washington, DC: American Psychiatric Association Publishing; 2022.
14. Kay SR, Fiszbein A, Opler LA. The positive and negative syndrome scale (PANSS) for schizophrenia. Schizophr Bull. 1987;13(2):261–76.
15. Mazhari S, Parvaresh N, Eslami Shahrbabaki M, Sadeghi MM, Nakhaee N, Keefe RSE. Validation of the Persian version of the brief assessment of cognition in schizophrenia in patients with schizophrenia and healthy controls. Psychiatry Clin Neurosci. 2014;68(2):160–6.
16. Whitfield-Gabrieli S, Nieto-Castanon A. Conn: a functional connectivity toolbox for correlated and anticorrelated brain networks. Brain Connect. 2012;2(3):125–41.
17. Nieto-Castanon A, Whitfield-Gabrieli S. CONN functional connectivity toolbox: RRID $SCR_0$09550, $release$22 : $HilbertPress$;2022.$StatisticalParametricMapping$: $TheAnalysisofFunctionalBrainImages$: $AcademicPress$;2007.

This open-access article distributed under the terms of the Creative Commons Attribution NonCommercial 3.0 License (CC BY-NC 3.0).
Downloaded from: https://journals.sbmu.ac.ir/aaem/index.php/AAEM/index

19. Ashburner J, Friston KJ. Unified segmentation. Neuroimage. 2005;26(3):839–51.
20. Ashburner J. A fast diffeomorphic image registration algorithm. Neuroimage. 2007;38(1):95–113.
21. Nieto-Castanon A. Handbook of Functional Connectivity Magnetic Resonance Imaging Methods in CONN: Hilbert Press; 2020.
22. Hallquist MN, Hwang K, Luna B. The nuisance of nuisance regression: spectral misspecification in a common approach to resting-state fMRI preprocessing reintroduces noise and obscures functional connectivity. Neuroimage. 2013;82:208–25.
23. Behzadi Y, Restom K, Liau J, Liu TT. A component based noise correction method (CompCor) for BOLD and perfusion based fMRI. Neuroimage. 2007;37(1):90–101.
24. Chai XJ, Castañón AN, Öngür D, Whitfield-Gabrieli S. Anticorrelations in resting state networks without global signal regression. Neuroimage. 2012;59(2):1420–8.
25. Nieto-Castanon A. Preparing fMRI Data for Statistical Analysis. arXiv. 2022.
26. Desikan RS, Ségonne F, Fischl B, Quinn BT, Dickerson BC, Blacker D, et al. An automated labeling system for subdividing the human cerebral cortex on MRI scans into gyral based regions of interest. Neuroimage. 2006;31(3):968–80.
27. Friston KJ, Buechel C, Fink GR, Morris J, Rolls E, Dolan RJ. Psychophysiological and modulatory interactions in neuroimaging. Neuroimage. 1997;6(3):218–29.
28. McLaren DG, Ries ML, Xu G, Johnson SC. A generalized form of context-dependent psychophysiological interactions (gPPI): a comparison to standard approaches. Neuroimage. 2012;61(4):1277–86.
29. Hyvärinen A. Fast and robust fixed-point algorithms for independent component analysis. IEEE Trans Neural Netw. 1999;10(3):626–34.
30. Jafri MJ, Pearlson GD, Stevens M, Calhoun VD. A method for functional network connectivity among spatially independent resting-state components in schizophrenia. Neuroimage. 2008;39(4):1666–81.
31. Sørensen T. A method of establishing groups of equal amplitude in plant sociology based on similarity of species content and its application to analyses of the vegetation on Danish commons. K Dan Vidensk Selsk Biol Skr. 1948;5(4):1–34.
32. Benjamini Y, Hochberg Y. Controlling the false discovery rate: a practical and powerful approach to multiple testing. J R Stat Soc B. 1995;57(1):289–300.
33. Yang R, He L, Zhang Z, Zhou W, Liu J. The Higher Parietal Cortical Thickness in Abstinent Methamphetamine Patients Is Correlated With Functional Connectivity and Age of First Usage. Front Hum Neurosci. 2021;15:705863.
34. Thompson PM, Hayashi KM, Simon SL, Geaga JA, Hong MS, Sui Y, et al. Structural abnormalities in the brains of human subjects who use methamphetamine. J Neurosci. 2004;24(26):6028–36.
35. Zilverstand A, Huang AS, Alia-Klein N, Goldstein RZ. Neuroimaging Impaired Response Inhibition and Salience Attribution in Human Drug Addiction: A Systematic Review. Neuron. 2018;98(5):886–903.
36. Van Der Plas EAA, Crone EA, Van Den Wildenberg WPM, Tranel D, Bechara A. Executive control deficits in substance-dependent individuals: a comparison of alcohol, cocaine, and methamphetamine and of men and women. J Clin Exp Neuropsychol. 2009;31(6):706–19.
37. Hu X, Jiang P, Gao Y, Sun J, Zhou X, Zhang L, et al. Brain morphometric abnormalities and their associations with affective symptoms in males with methamphetamine use disorder during abstinence. Front Psychiatry. 2022;13:1003889.
38. Zhang S, Hu Q, Tang T, Liu C, Li C, Zang YY, et al. Changes in gray matter density, regional homogeneity, and functional connectivity in methamphetamine-associated psychosis: a resting-state functional magnetic resonance imaging (fMRI) study. Med Sci Monit. 2018;24:4020–30.
39. Tian Y, Wang D, Fan F, Yang Y, Fu F, Wei D, et al. Differences in cognitive deficits in patients with methamphetamine and heroin use disorder compared with healthy controls in a Chinese Han population. Prog Neuropsychopharmacol Biol Psychiatry. 2022;117:110543.
40. Li Y, Wang X, Huang S, Huang Q, Yang R, Liao Z, et al. Hyperconnectivity of the lateral amygdala in long-term methamphetamine abstainers negatively correlated with withdrawal duration. Front Pharmacol. 2023;14:1138704.
41. Wang L, Hu F, Wang W, Li Q, Li Y, Zhu J, et al. Altered brain intrinsic functional hubs and connectivity associated with relapse risk in heroin dependents undergoing methadone maintenance treatment: a resting-state fMRI study. Drug Alcohol Depend. 2021;219:108503.
42. Kirby KN, Petry NM, Bickel WK. Heroin addicts have higher discount rates for delayed rewards than non-drug-using controls. J Exp Psychol Gen. 1999;128(1):78–87.
43. Zhu J, Wang S, Liu Y, Wang F, Li Q, Li Z, et al. The influence of methadone on cerebral gray matter and functional connectivity. Ann Palliat Med. 2021;10(9):9497–507.
44. Zhang R, Volkow ND. Brain default-mode network dysfunction in addiction. Neuroimage. 2019;200:313–31.
45. Lerman C, Gu H, Loughead J, Ruparel K, Yang Y, Stein EA. Large-scale brain network coupling predicts acute nicotine abstinence effects on craving and cognitive function. JAMA Psychiatry. 2014;71(5):523–30.
46. Chawla M, Garrison KA. Neurobiological Considerations for Tobacco Use Disorder. Curr Behav Neurosci Rep. 2018;5(4):238–48.
47. Zhang H, Hu Y, Yu Y, Zhou Z, Sun Y, Qi C, et al. The value of multimodal neuroimaging in the diagnosis and treatment of post-traumatic stress disorder: a narrative review. Transl Psychiatry. 2025;15:208.
48. Wang L, Hu W, Wang H, Song Z, Lin H, Jiang J. Differ-

This open-access article distributed under the terms of the Creative Commons Attribution NonCommercial 3.0 License (CC BY-NC 3.0).
Downloaded from: https://journals.sbmu.ac.ir/aaem/index.php/AAEM/index

ent stimulation targets of rTMS modulate specific triple-network and hippocampal-cortex functional connectivity. Brain Stimul. 2024;17(6):1256–64.

This open-access article distributed under the terms of the Creative Commons Attribution NonCommercial 3.0 License (CC BY-NC 3.0).
Downloaded from: https://journals.sbmu.ac.ir/aaem/index.php/AAEM/index

Table 1: Demographic characteristics of study participants (N = 10,000)

Variable	HC (n=35)	METH (n=45)	MMT (n=30)	P	η^2	METH vs. MMT
Age (years)						
Mean ± SD	35.70 ± 7.97	34.00 ± 7.54	34.50 ± 8.03	0.80	0.009	-0.06 (-0.53, 0.40)
Education (years)						
Mean ± SD	11.80 ± 2.40	10.90 ± 2.50	11.10 ± 2.30	0.21	0.026	-0.08 (-0.54, 0.38)
Duration of dependence (years)†						
Mean ± SD	—	5.50 ± 2.80	5.20 ± 2.60	0.62	0.003	0.11 (-0.35, 0.57)
BACS Composite Score						
Mean ± SD	30.38 ± 5.85	19.88 ± 6.20	22.48 ± 7.61	0.002	0.332	-0.38 (-0.85, 0.08)
Tests						
Verbal memory	39.57 ± 10.95	31.37 ± 10.94	32.44 ± 7.22	0.013	0.119	-0.11 (-0.57, 0.35)
Serial number test	15.40 ± 4.75	12.60 ± 5.25	13.02 ± 5.18	0.015	0.058	-0.08 (-0.54, 0.38)
Verbal fluency	16.36 ± 4.19	15.96 ± 6.63	16.87 ± 5.45	0.20	0.004	-0.15 (-0.61, 0.32)
Token motor test	54.14 ± 2.94	34.25 ± 2.90	40.53 ± 3.77	0.008	0.880	-1.92 (-2.48, -1.36)
PANSS						
Positive	8.86 ± 1.59	23.10 ± 3.07	14.80 ± 2.96	<0.001	0.844	2.74 (2.10, 3.38)
Negative	9.52 ± 1.89	22.15 ± 3.24	15.34 ± 2.64	<0.001	0.802	2.26 (1.67, 2.85)
General psychopathology	18.76 ± 1.35	46.44 ± 6.13	36.46 ± 6.00	<0.001	0.913	1.64 (1.11, 2.18)

Data are presented as mean ± standard deviation (SD) or 95% confidence interval. HC: healthy controls;
METH: untreated methamphetamine users; MMT: methadone maintenance therapy receivers; BACS: Brief Assessment of Cognition in Schizophrenia; PANSS: Positive and Negative Syndrome Scale.
† Duration of dependence applies only to participants with methamphetamine use disorder.
Participants receiving methadone maintenance therapy were treated with a stable dose of 60–90 mg/day (mean 72 ± 15 mg/day).

This open-access article distributed under the terms of the Creative Commons Attribution NonCommercial 3.0 License (CC BY-NC 3.0).
Downloaded from: https://journals.sbmu.ac.ir/aaem/index.php/AAEM/index

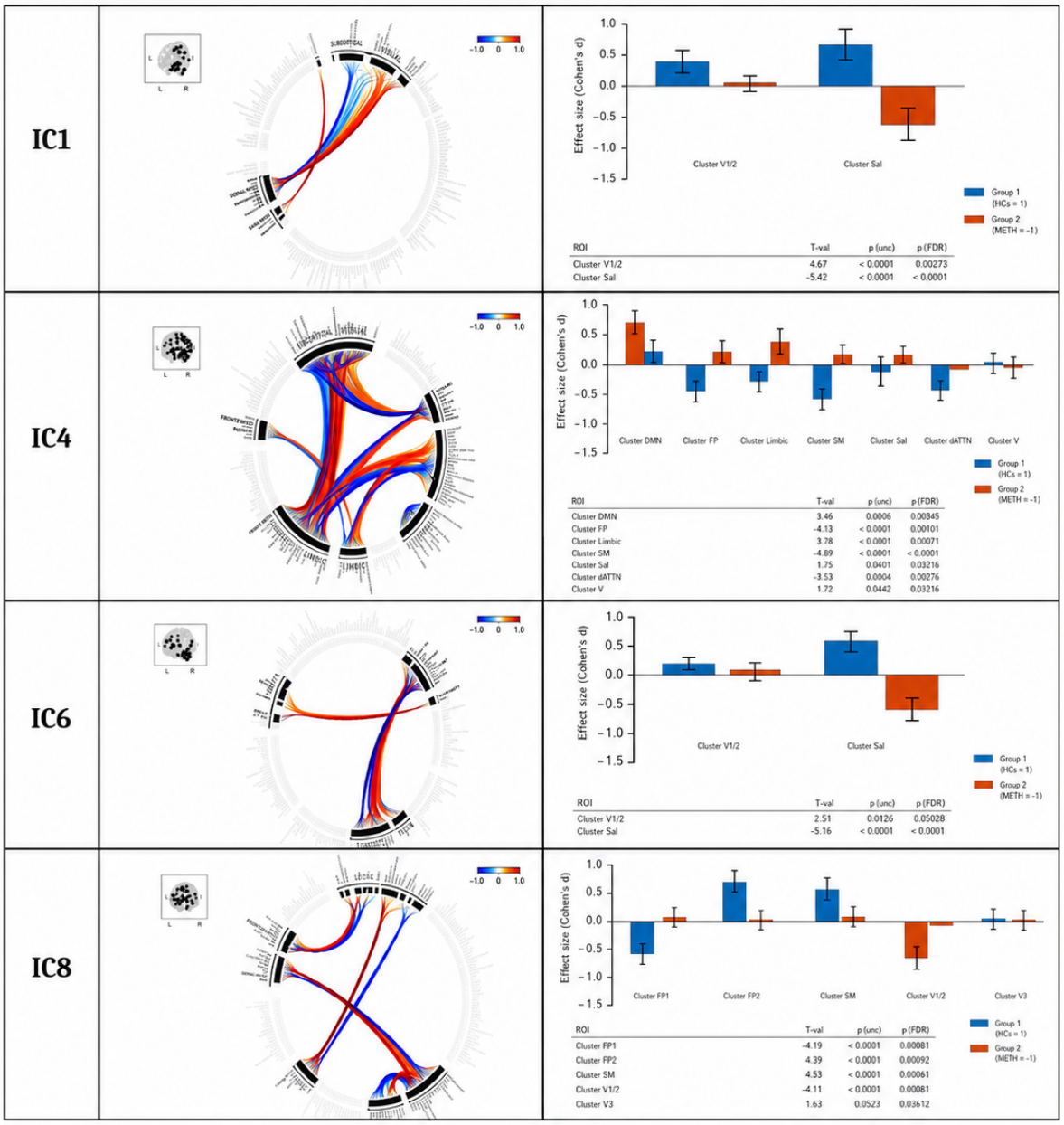

Figure 1: Dynamic independent component (dICA) analysis: the ROI-to-ROI connectivity circle diagram across 10 IC spatial components. Between-group contrasts (HC = 1 vs. METH = -1) revealed significant differences in IC1, IC4, IC6, and IC8, with corresponding effect sizes shown for each cluster ($p < 0.05$, FDR-corrected). HC: healthy controls; METH: untreated methamphetamine users; IC: independent component; ROI: region of interest; FDR: false discovery rate.

IC1: Hippocampal–dorsal attention–sensorimotor and posterior default-mode/visual circuit

IC4: Visual–occipital–cerebellar and medial prefrontal/cingulate circuit

IC6: Frontoparietal–temporal-fusiform–parahippocampal circuit

IC8: Lateral sensorimotor–language–superior temporal circuit.

This open-access article distributed under the terms of the Creative Commons Attribution NonCommercial 3.0 License (CC BY-NC 3.0).
Downloaded from: https://journals.sbmu.ac.ir/aaem/index.php/AAEM/index

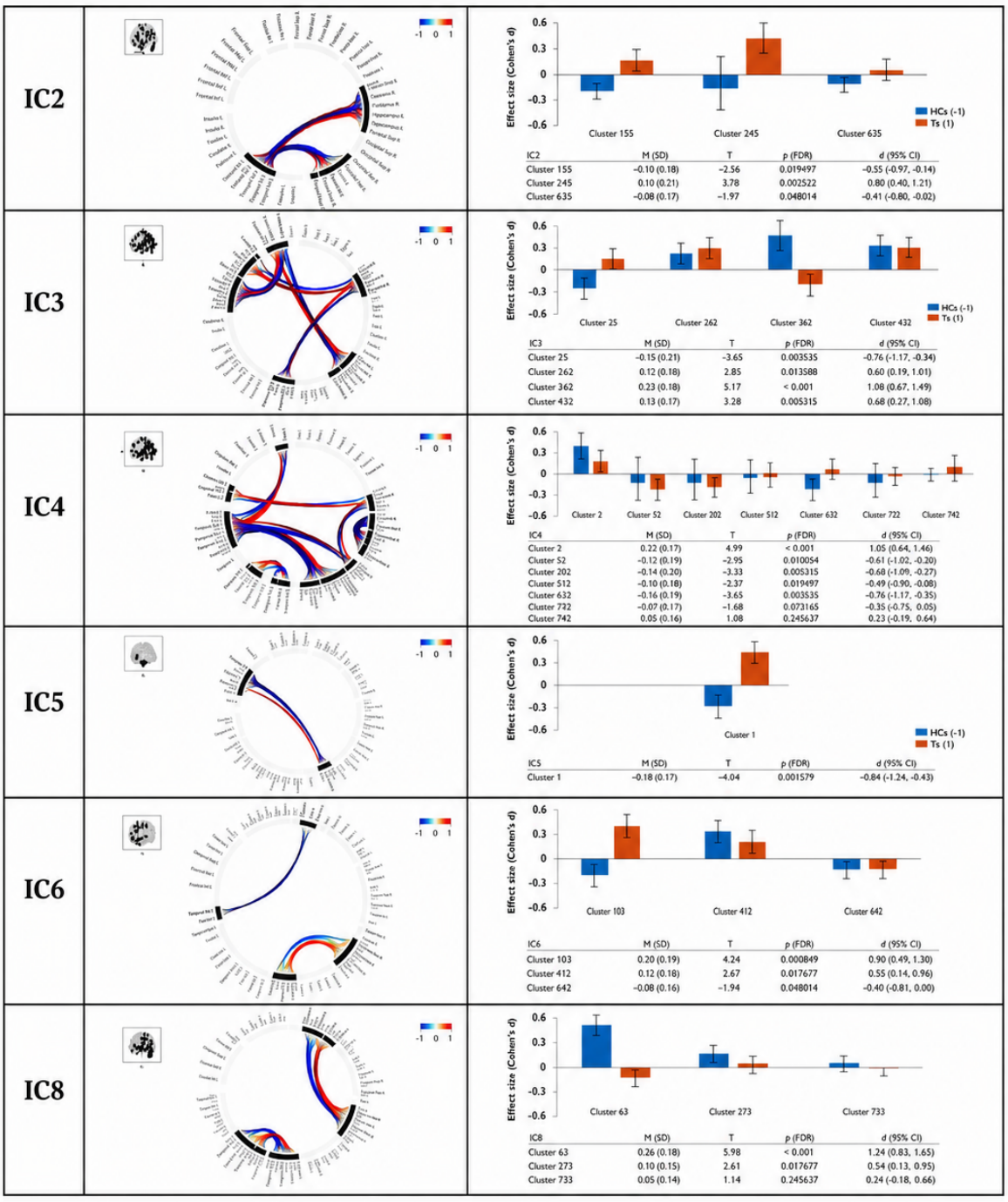

Figure 2: Dynamic independent component analysis (dICA): the ROI-to-ROI connectivity circle diagram across 10 spatial ICs. Between-group contrasts (HC = 1 vs. MMT = -1) revealed significant differences in IC2, IC3, IC4, IC5, IC6, and IC8, with corresponding effect sizes for each cluster ($p < 0.05$, FDR-corrected). HC: healthy controls; MMT: MMT-treated participants; IC: independent component; ROI: region of interest; FDR: false discovery rate; CI: confidence interval.

IC2: Default-mode–hippocampal/medial temporal circuit, primarily involving the posterior cingulate cortex, precuneus, and hippocampal regions. IC3: Salience–limbic/interoceptive circuit, involving systems related to affective regulation and internal-state processing. This is an operational label based on the network pattern and its interpretation in the manuscript.

IC4: Visual–occipital–cerebellar and medial prefrontal/cingulate circuit.

IC5: Visual–cerebellar circuit, reflecting connectivity involved in visual integration, cerebellar processing, and motor sequencing.

IC6: Frontoparietal–temporal fusiform–parahippocampal circuit.

IC8: Lateral sensorimotor–language–superior temporal circuit, including language-related regions, posterior superior temporal gyrus, and superior temporal gyrus.

This open-access article distributed under the terms of the Creative Commons Attribution NonCommercial 3.0 License (CC BY-NC 3.0).
Downloaded from: https://journals.sbmu.ac.ir/aaem/index.php/AAEM/index

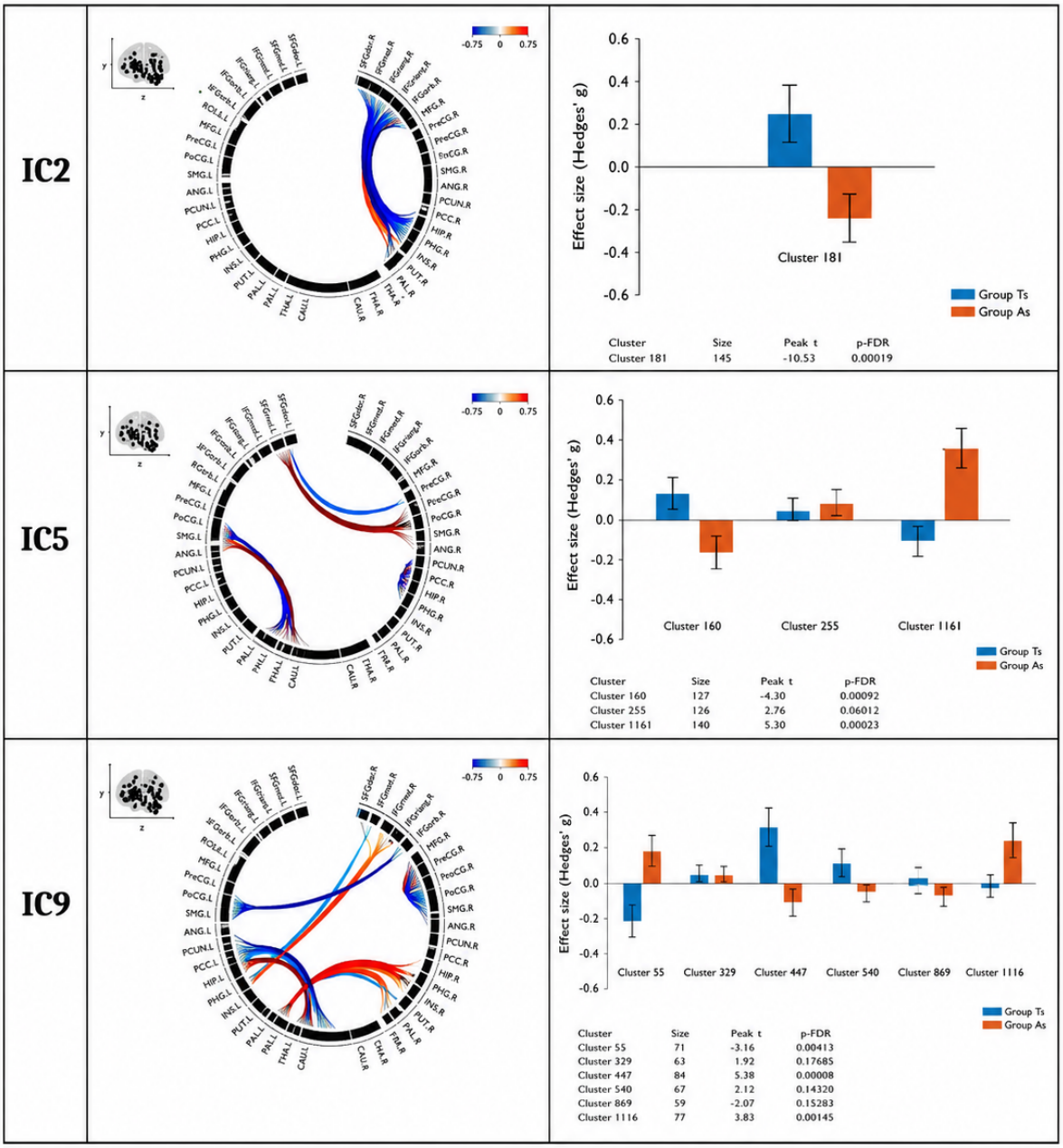

Figure 3: Dynamic independent component analysis (dICA): the ROI-to-ROI connectivity circle diagram across 10 spatial ICs. Between-group contrasts (MMT = 1 vs. METH = -1) revealed significant differences in IC2, IC5, and IC9, with corresponding effect sizes for each cluster ($p < 0.05$, FDR-corrected). METH: untreated methamphetamine users; MMT: methadone maintenance treatment group; IC: independent component; ROI: region of interest; FDR: false discovery rate.

IC2: A default-mode–hippocampal/medial temporal circuit, primarily involving the posterior cingulate cortex, precuneus, hippocampus, and related medial temporal regions.

IC5: A visual–cerebellar/sensorimotor integration circuit, reflecting interactions involved in visuospatial processing, sensory integration, and motor coordination.

IC9: A frontostriatal–limbic–sensorimotor integration circuit, involving prefrontal and parietal regions together with the insula, basal ganglia, hippocampal/parahippocampal regions, and posterior midline structures. IC9 was one of the components distinguishing MMT-treated from untreated METH participants.

This open-access article distributed under the terms of the Creative Commons Attribution NonCommercial 3.0 License (CC BY-NC 3.0).
Downloaded from: https://journals.sbmu.ac.ir/aaem/index.php/AAEM/index